Anal. Chem. **2001,** *73,* 565−570

Single-Molecule DNA Amplification and Analysis in an Integrated Microfluidic Device

E. T. Lagally,[†] I. Medintz,[‡] and R. A. Mathies*[,†,‡]

Department of Chemistry, University of California, Berkeley, California 94720

Stochastic PCR amplification of single DNA template molecules followed by capillary electrophoretic (CE) analysis of the products is demonstrated in an integrated microfluidic device. The microdevice consists of submicroliter PCR chambers etched into a glass substrate that are directly connected to a microfabricated CE system. Valves and hydrophobic vents provide controlled and sensorless loading of the 280-nL PCR chambers; the low volume reactor, the low thermal mass, and the use of thin-film heaters permit cycle times as fast as 30 s. The amplified product, labeled with an intercalating fluorescent dye, is directly injected into the gel-filled capillary channel for electrophoretic analysis. Repetitive PCR analyses at the single DNA template molecule level exhibit quantized product peak areas; a histogram of the normalized peak areas reveals clusters of events caused by 0, 1, 2, and 3 viable template copies in the reactor and these event clusters are shown to fit a Poisson distribution. This device demonstrates the most sensitive PCR possible in a microfabricated device. The detection of single DNA molecules will also facilitate single-cell and single-molecule studies to expose the genetic variation underlying ensemble sequence and expression averages.

The polymerase chain reaction (PCR) has revolutionized bioscience because of its ability to exponentially and specifically amplify DNA templates from very small starting concentrations.[1] The theoretical template concentration limit of PCR is a single molecule, and stochastic amplification from single DNA templates has been demonstrated.[2−5] The specificity of PCR plays an increasingly important role at these low template concentrations, where the ability to selectively amplify a single target sequence from a larger genetic background is critical. Since PCR is typically performed in large-microliter volumes, it is necessary to work with very low (∼10^{-18} M) concentrations to approach the single-molecule limit.

The advent of biological microdevices[6] allows one to consider conducting bioanalytical assays such as PCR at very small volumes to increase the speed of these assays and to reduce the amount of material and reagents needed. Our own work in this area has included DNA fragment sizing and sequencing on capillary and capillary array electrophoresis microdevices,[7,8] integrated electrochemical detection,[9] and amino acid chirality analysis.[10] The first microfabricated PCR reactors were constructed from silicon and glass and amplified DNA from template concentrations down to roughly 2000 copies/μL, in volumes down to 1 μL.[11] Since then, stand-alone PCR reactors have been constructed in silicon,[12−15] glass,[16−18] and fused-silica capillaries.[19] Most designs use resistive heaters surrounding the chambers, but some designs utilize noncontact methods[16] or continuous flow through three differentially heated regions.[18] Unfortunately, most of these designs either require bulk heating,[16,17] making parallel analyses with different thermal cycling profiles difficult, or require large starting concentrations or large sample volumes.[18] Furthermore, typically the sample must be manually transferred to an analysis device, introducing external contamination and increasing the time needed for the assay.

Integrated systems combining rapid thermal cycling PCR amplification with capillary electrophoretic (CE) analysis address

* Corresponding author: (fax) 510 642-3599; (e-mail) rich@zinc.cchem.berkeley.edu.

[†] UCB/UCSF Joint Bioengineering Graduate Group.

[‡] Department of Chemistry.

(1) Mullis, K.; Faloona, F.; Scharf, S.; Saiki, R.; Horn, G.; Erlich, H. *Cold Spring Harbor Symp. Quant. Biol.* **1986**, *51*, 263−273.
(2) Li, H. H.; Gyllensten, U. B.; Cui, X. F.; Saiki, R. K.; Erlich, H. A.; Arnheim, N. *Nature* **1988**, *335*, 414−417.
(3) Saiki, R. K.; Gelfand, D. H.; Stoffel, S.; Scharf, S. J.; Higuchi, R.; Horn, G. T.; Mullis, K. B.; Erlich, H. A. *Science* **1988**, *239*, 487−491.
(4) Zhang, L.; Cui, X. F.; Schmitt, K.; Hubert, R.; Navidi, W.; Arnheim, N. *Proc. Natl. Acad. Sci. U.S.A.* **1992**, *89*, 5847−5851.
(5) Ohuchi, S.; Nakano, H.; Yamane, T. *Nucleic Acids Res.* **1998**, *26*, 4339−4346.
(6) van den Berg, A.; Olthuis, W.; Bergveld, T. *Micro Total Analysis Systems 2000*; Kluwer Academic Publishers: Dordrecht, The Netherlands, 2000.
(7) Liu, S. R.; Shi, Y. N.; Ja, W. W.; Mathies, R. A. *Anal. Chem.* **1999**, *71*, 566−573.
(8) Shi, Y. N.; Simpson, P. C.; Scherer, J. R.; Wexler, D.; Skibola, C.; Smith, M. T.; Mathies, R. A. *Anal. Chem.* **1999**, *71*, 5354−5361.
(9) Woolley, A. T.; Lao, K. Q.; Glazer, A. N.; Mathies, R. A. *Anal. Chem.* **1998**, *70*, 684−688.
(10) Hutt, L. D.; Glavin, D. P.; Bada, J. L.; Mathies, R. A. *Anal. Chem.* **1999**, *71*, 4000−4006.
(11) Cheng, J.; Shoffner, M. A.; Hvichia, G. E.; Kricka, L. J.; Wilding, P. *Nucleic Acids Res.* **1996**, *24*, 380−385.
(12) Wilding, P.; Kricka, L. J.; Cheng, J.; Hvichia, G.; Shoffner, M. A.; Fortina, P. *Anal. Biochem.* **1998**, *257*, 95−100.
(13) Chaudhari, A. M.; Woudenberg, T. M.; Albin, M.; Goodson, K. E. *J. Microelectromech. Syst.* **1998**, *7*, 345−355.
(14) Daniel, J. H.; Iqbal, S.; Millington, R. B.; Moore, D. F.; Lowe, C. R.; Leslie, D. L.; Lee, M. A.; Pearce, M. J. *Sens. Actuators, A* **1998**, *71*, 81−88.
(15) Northrup, M. A.; Benett, B.; Hadley, D.; Landre, P.; Lehew, S.; Richards, J.; Stratton, P. *Anal. Chem.* **1998**, *70*, 918−922.
(16) Oda, R. P.; Strausbauch, M. A.; Huhmer, A. F. R.; Borson, N.; Jurrens, S. R.; Craighead, J.; Wettstein, P. J.; Eckloff, B.; Kline, B.; Landers, J. P. *Anal. Chem.* **1998**, *70*, 4361−4368.
(17) Taylor, T. B.; Harvey, S. E.; Albin, M.; Lebak, L.; Ning, Y.; Mowat, I.; Schuerlein, T.; Principe, E. *Biomed. Microdevices* **1998**, *1*, 65−70.
(18) Kopp, M. U.; de Mello, A. J.; Manz, A. *Science* **1998**, *280*, 1046−1048.
(19) Zhang, N. Y.; Tan, H. D.; Yeung, E. S. *Anal. Chem.* **1999**, *71*, 1138−1145.

10.1021/ac001026b CCC: $20.00
Published on Web 01/03/2001

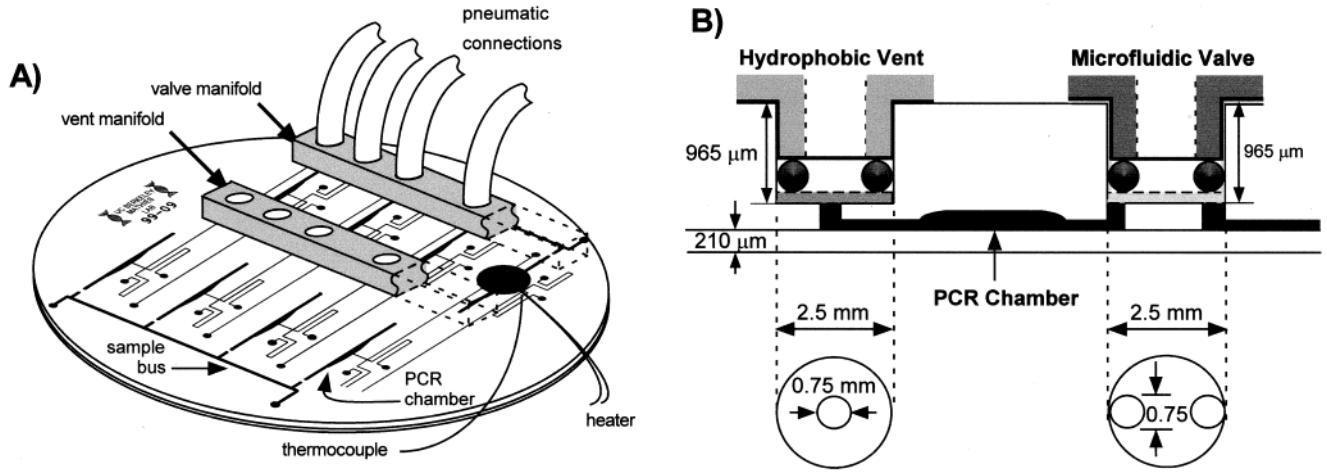

Figure 1. (A) Microfluidic PCR−CE device. The PCR chambers are connected to a common sample bus through a set of valves. Hydrophobic vents at the other end of the PCR chambers are used to locate the sample and to eliminate gas. The PCR chambers are directly connected to the cross channel of the CE system for product injection and analysis. Two aluminum manifolds, one each for the vents and valves, are placed onto the respective ports and clamped in place using vacuum. The manifolds connect to external solenoid valves for pressure and vacuum actuation. Thermal cycling is accomplished using a resistive heater and a miniature thermocouple below the 280-nL chamber. (B) Detailed schematic of microfluidic valves and hydrophobic vents. Sample is loaded from the right by opening the valve using vacuum (30 mmHg) and forcing the sample under the membrane using pressure (10−12 psi); vacuum is simultaneously applied at the vent to evacuate the air from the chamber. The sample stops at the vent, and the valve is pressure-sealed to enclose the sample. Dead volumes for the valves and vents are ~50 nL.

most of the problems outlined above. In previous work, we developed two generations of small-volume PCR chambers integrated with glass CE microdevices.[20,21] The first integrated PCR−CE device used 10-μL silicon chambers with polysilicon heaters that were attached to a glass CE microchannel.[21] This device was capable of amplifying 4×10^5 template copies/μL in a time of 15 min. Later work from other laboratories utilizing Peltier elements for thermal cycling have been successful, but have not shown a significant time or sensitivity advantage over conventional thermal cycling systems.[22−24] An integrated microdevice utilizing submicroliter sample volumes with sensitivity to the single-molecule limit would avoid these shortcomings and could serve as a platform for high-throughput parallelization.

Toward this goal, we have focused on the development of a monolithically integrated PCR−CE device. Our current design includes 280-nL PCR chambers etched into a glass substrate, connected to microfluidic valves and hydrophobic vents for sample introduction and immobilization during thermal cycling.[20] This work was inspired by the valve/vent technologies shown by Anderson et al.;[25] however, that fabrication technology was targeted to microliter volumes, while our integrated PCR−CE system required sample volumes in the nanoliter range. Microfluidic valve and hydrophobic vent technology was thus developed with 50−100-nL dead volumes to enable the precise loading and containment of submicroliter samples. This device demonstrated an excellent detection sensitivity down to 20 copies/μL and fast amplifications (30 s/cycle). These capabilities suggested that it might be possible to perform stochastic single-molecule PCR amplification.

Here we present an extensive series of PCR−CE chip experiments at very low concentrations of target to explore the stochastic amplification of single DNA molecule templates. A statistically significant number of trials are performed and analyzed with calculations of normalized peak areas between the single-molecule product and an internal amplification control. The event amplitudes and frequencies at a mean occupancy of ~1 template molecule in the reactor are found to conform to a Poisson distribution, demonstrating that we are operating at the single-molecule level. The capability of amplifying single-copy templates combined with microfluidic integration will facilitate the development of enhanced microfluidic diagnostic devices as well as studies of single-cell genetic phenomena and expression variation.

EXPERIMENTAL SECTION

Microfabrication. Figure 1A presents the mask design used to create the microfluidic PCR−CE chips. Microfabrication of the PCR−CE devices is described in depth elsewhere.[20,26] Briefly, glass wafers (1.1 mm thick D263, Schott, Yonkers, NY) were coated with a 2000-Å layer of amorphous silicon using low-pressure chemical vapor deposition (LPCVD). The wafers were primed with hexamethyldisilazane, spin-coated with photoresist (Shipley 1818, Marlborough, MA), and then soft-baked. The mask pattern was transferred to the substrate by exposing the photoresist in a Quintel UV contact mask aligner. The photoresist was developed in a 1:1 mixture of Microposit developer concentrate

(20) Lagally, E. T.; Simpson, P. C.; Mathies, R. A. *Sens. Actuators, B* **2000**, *63*, 138−146.
(21) Woolley, A. T.; Hadley, D.; Landre, P.; deMello, A. J.; Mathies, R. A.; Northrup, M. A. *Anal. Chem.* **1996**, *68*, 4081−4086.
(22) Dunn, W. C.; Jacobson, S. C.; Waters, L. C.; Kroutchinina, N.; Khandurina, J.; Foote, R. S.; Justice, M. J.; Stubbs, L. J.; Ramsey, J. M. *Anal. Biochem.* **2000**, *277*, 157−160.
(23) Waters, L. C.; Jacobson, S. C.; Kroutchinina, N.; Khandurina, J.; Foote, R. S.; Ramsey, J. M. *Anal. Chem.* **1998**, *70*, 5172−5176.
(24) Khandurina, J.; McKnight, T. E.; Jacobson, S. C.; Waters, L. C.; Foote, R. S.; Ramsey, J. M. *Anal. Chem.* **2000**, *72*, 2995−3000.
(25) Anderson, R. C.; Bogdan, G. J.; Barniv, Z.; Dawes, T. D.; Winkler, J.; Roy, K. In *Proc. 1997 International Conference on Solid-State Sensors and Actuators* (Transducers '97); IEEE: Chicago, IL, 1997; pp 477−480.
(26) Simpson, P. C.; Woolley, A. T.; Mathies, R. A. *J. Biomed. Microdevices* **1998**, *1*, 7−26.

and H_2O. The sacrificial silicon layer was etched using a SF_6 plasma in a parallel-plate reactive ion etching (RIE) system (Plasma-Therm, St. Petersburg, FL), and the fluidic channels, electrophoresis channels, and 280-nL PCR chambers were etched 42 μm deep in buffered HF acid. The remaining silicon was stripped using an SF_6 plasma, and the wells at the cathode, anode, and waste locations were drilled using a rotary drill press. The etched substrate contains eight analysis units consisting of a PCR chamber, a valve, a vent, and a CE microchannel. Valve and vent structures (see Figure 1B) were formed by drilling a hole to a depth of 965 μm from the back of the etched plate with a 2.5-mm-diameter diamond-tipped drill bit (Crystalite, Westerville, OH). The valve and vent ports were then drilled through the substrate to the channels using a 0.75-mm-diameter diamond-tipped bit. The drilled wafer was thermally bonded to a 210-μm cover plate using a programmable vacuum furnace (Centurion VPM, J.M. Ney, Yucaipa, CA). The channel surfaces were coated using a modified version of the Hjerten coating protocol.[27]

After fabrication, 1-cm^2 resistive heaters (Minco HK5537, Minneapolis, MN) and miniature T-type thermocouples (Omega 5TC-TT, Stamford, CT) were applied to the back of the device using silicone heat sink compound and secured with polyimide tape. The valves and vents were actuated using aluminum pneumatic manifolds that vacuum clamp to the chip during use. Pressure and vacuum controlled from external solenoid valves are used to actuate the microfluidic elements. Latex membranes (2.5-mm diameter, thickness ~150 μm) were attached to 2.5-mm-o.d. O-rings (Apple Rubber Products, Lancaster, NY) with epoxy, and the structures were placed around the projections on the valve manifold. Hydrophobic vent material consisting of circular sections of a 1.0-μm-pore size hydrophobic membrane (Millipore, Bedford, MA) were installed concurrently. The dead volumes for the hydrophobic vents are ~50 nL; the valves have two ports instead of one, so the total dead volume is 100 nL, but only one port is filled with sample during operation, making the effective dead volume ~50 nL.

Instrumentation. The PCR chambers were thermally cycled with a program written in LabVIEW (National Instruments, Austin, TX). Thermocouple input voltages passed through a signal conditioning unit (National Instruments 5B backplane) and into a 12-bit ADC card running on a Macintosh Performa 6400 computer. Temperature control was accomplished through a percentage/integrator/differentiator (PID) module within the LabVIEW program. The DAC output used to control the heater passed through a current source circuit to supply the power necessary to drive the heaters.

The PCR−CE chips were prepared for operation by forcing the separation medium through the entire microfluidic system using a syringe. The CE separation medium consisted of 0.75% (w/v) hydroxyethyl cellulose (HEC) in 1× Tris acetate EDTA (TAE) buffer with 1 μM thiazole orange. The gel was then evacuated from the PCR chambers and the sample bus by applying vacuum at the valve reservoir, forming a passive barrier to the flow of reagents from the PCR chamber into the separation channel during amplification.[21] The valve and vent manifolds were clamped to the chip, and the sample was introduced at one of the sample bus reservoirs with a pipet. The valve was opened by applying vacuum to the appropriate port on the valve manifold, and vacuum was simultaneously applied to the corresponding hydrophobic vent. Air pressure applied at the sample bus forced the sample through the valve and into the PCR chamber. The valve was then pressure-sealed (10−15 psi) to prevent sample movement during heating. Bubble-free loading was consistently achieved using this methodology.

PCR Amplification and Capillary Electrophoresis. The templates for multiplex PCR amplification consisted of a 136-bp amplification product derived from the M13/pUC19 cloning vector (New England Biolabs, Beverly, MA) and a 231-bp product amplified from a human genomic DNA control sample (Centre d′Estude du Polymorphisme Humain, (CEPH) DNA, Coriell Cell Repositories, Camden, NJ).[28] The primers for the 231-bp amplification product define the S65C wild-type-specific allele in the *HFE* gene (*HLA6*) associated with hereditary haemochromatosis.[28,29] The sequences (S65C forward = 5′TCCCCTCCTACTACACATGG 3′ T_m = 49 °C, S65C reverse = 5′TCAGCTGCAGCCACATCTGGC 3′ T_m = 53 °C) are adapted from a set of primers used in our laboratory to assay an A → T variation at nucleotide 193 on exon 2 of the *HFE* gene.[30,31] The primers specific to the M13 template were the M13/pUC19 forward and reverse primers (forward = 5′CCCAGTCACGACGTTGTAAAACG3′ T_m = 56 °C, reverse = 5′AGCGGATAACAATTTCACACAGG 3′ T_m = 56 °C). The template DNA for the stochastic amplifications consisted of a serial dilution of the entire 2686-bp M13/pUC19 cloning vector. A dilution of the 231-bp HFE amplicon, obtained using a conventional thermal cycler (MJ Research, Watertown, MA), was used as a control. The PCR mixture (50 μL) consisted of Taq MasterMix kit (1× PCR buffer, 1.5 mM $MgCl_2$, 200 μM each dNTP, and 2.5 units of *Taq* polymerase, Qiagen, Valencia, CA), 1.5 μM BSA, 0.2 μM each M13/pUC forward and M13/pUC reverse primer, 0.25 μM each S65C forward and S65C reverse primer, and approximately 200 copies of M13 template and 1000 copies of S65C template. The solution was made fresh daily and kept on ice. The on-chip thermal cycling program employed a "touchdown" PCR protocol,[32] consisting of a 1-min hold at 95 °C to fully denature the templates, followed by a series of 2 cycles each at successively lower annealing temperatures, followed by 15 cycles of amplification using the lowest annealing temperature. The annealing temperatures started at 64 °C and dropped in increments of 2 °C until reaching 50 °C; the denaturing and extension temperatures were 94 and 72 °C, respectively. The use of a 210-μm backplate on our device with active cooling using nitrogen flowing over the top of the chip allowed for heating and cooling rates of ~10 °C/s.[20] Each cycle had step times of 5 s at the denaturation temperature, 15 s at the annealing temperature, and 10 s at the extension temperature, for a total run time of 15 min (30 cycles).

(27) Hjerten, S. *J. Chromatogr.* **1985**, *347*, 191−198.

(28) Medintz, I.; Wong, W. W.; Sensabaugh, G.; Mathies, R. A. *Electrophoresis* **2000**, *21*, 2352−2358.

(29) Mura, C.; Nousbaum, J.-B.; Verger, P.; Moalic, M.-T.; Raguenes, O.; Mercier, A.-Y.; Ferec, C. *Hum. Genet.* **1997**, *101*, 271−276.

(30) Beutler, E.; Gelbart, T.; West, C.; Lee, P.; Adams, M.; Blackstone, R.; Pockros, P.; Kosty, M.; Venditti, C. P.; Phatak, P. D.; Seese, N. K.; Chorney, K. A.; TenElshof, A. E.; Gerhard, G. S.; Chorney, M. *Blood Cells Mol. Dis.* **1996**, *22*, 187−194.

(31) Jouanolle, A. M.; Gandon, G.; Jezequel, P.; Blayau, M.; Campion, M. L.; Yaouanq, J.; Mosser, J.; Fergelot, P.; Chauvel, B.; Bouric, P.; Carn, G.; Andrieux, N.; Gicquel, I.; LeGall, J. Y.; David, V. *Nat. Genet.* **1996**, *14*, 251−252.

(32) Hecker, K. H.; Roux, K. H. *Biotechniques* **1996**, *20*, 478−485.

Following amplification, the valve manifold was removed from the chip to provide access for platinum electrodes and for the placement of 1× TAE run buffer in the anode, cathode, and waste reservoirs for injection and separation. After PCR amplification, 112 V/cm was applied for 10 s between the PCR chamber and the waste reservoir to inject the PCR product into the separation channel; separation was performed by applying 236 V/cm between the cathode and anode reservoirs. A 100-bp DNA sizing ladder (New England Biolabs) was used to verify the size of the PCR product.

Electrophoretic separations were detected with a laser-excited confocal fluorescence detection system as described previously.[21] Briefly, the chip was placed on a stage and the 488-nm line from an argon ion laser was focused on one of the separation channels at a position 4.6 cm from the injection cross. Fluorescence was collected by a 32× (0.4 NA) objective, spatially filtered by a 160-μm pinhole, spectrally filtered by a 515-nm band-pass dichroic filter (30-nm bandwidth), and detected by a photomultiplier.

Data Analysis. Areas for each electrophoretic product peak were calculated by fitting Gaussian distributions to each peak and then integrating under the distribution using IgorPro (WaveMetrics, Lake Oswego, OR). Poisson distributions were fit using Stat::Fit statistical software (Geer Mountain Software, South Kent, CT) and a generalized linear model (GLM) to calculate maximum likelihood estimates. Goodness-of-fit statistics were also generated using this software.

RESULTS AND DISCUSSION

As the number of target molecules for the PCR reaction is reduced toward unity, stochastic effects begin to appear, and repeated amplifications of nominally identical solutions will reveal single-molecule fluctuations. In particular, for repeated amplifications from a reaction mixture, quantum steps in the amount of final product will be produced due to the discrete number of template molecules present at the start of the reaction. The resulting distribution of event frequencies and amplitudes should conform to a Poisson distribution with parameter λ, equal to the mean number of template molecules before amplification.[3] Thus, repeated trials are needed to create a statistical population representative of the actual template concentration.

Figure 2 presents a selection of the 60 amplifications conducted, demonstrating a representative range of the results. In some amplifications, no 136-bp amplicon is seen, but the 231-bp control is present. In some amplifications, a small 136-bp peak is present as well as the 231-bp control peak. In the remaining amplifications, both peaks are present, but the ratio of the two has changed and the M13 peak dominates. In all amplifications, the control peak is present, demonstrating successful PCR. This control differentiates between a failed PCR and stochastic M13 amplification in cases where no M13 peak is seen. In every amplification where a 136-bp peak is present, the peak area of the 231-bp amplicon decreases. This is presumably due to competition between the two amplicons for resources during the PCR. The two DNA templates were intentionally selected to use different primers, both to minimize the possibility of competition for primers and to bias the reaction in favor of the M13 template. The ratio change seen may occur because the melting temperatures of the M13 primers are higher than those of the S65C control primers; the M13 therefore begins amplifying earlier in the touchdown protocol. In addition, the M13 template amplifies with a slightly higher efficiency due to its shorter length. As a result, for cases in which there are more initial M13 template molecules in the reactor, there will be a more rapid accumulation of M13 products that will compete for polymerase and other PCR reagents in later cycles. For amplification in the linear regime, a measure

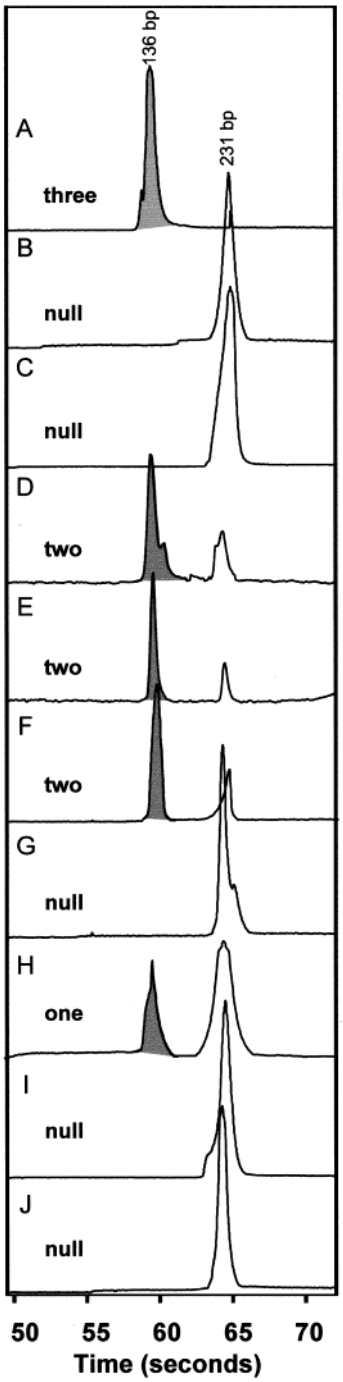

Figure 2. Ten representative electropherograms from a total of 60 PCR amplifications/analyses of single-molecule templates with internal controls. In each amplification, the 231-bp control peak is seen, indicating successful PCR amplification. In some of the amplifications (B, C, G, I, J) only the control peak is seen, in some amplifications a 136-bp peak is seen, but it is small in proportion to the control peak (H); in some the 136-bp peak is larger (D, E, F); and in some this peak dominates over the control peak (A). These 10 amplifications were conducted in this order over a single day.

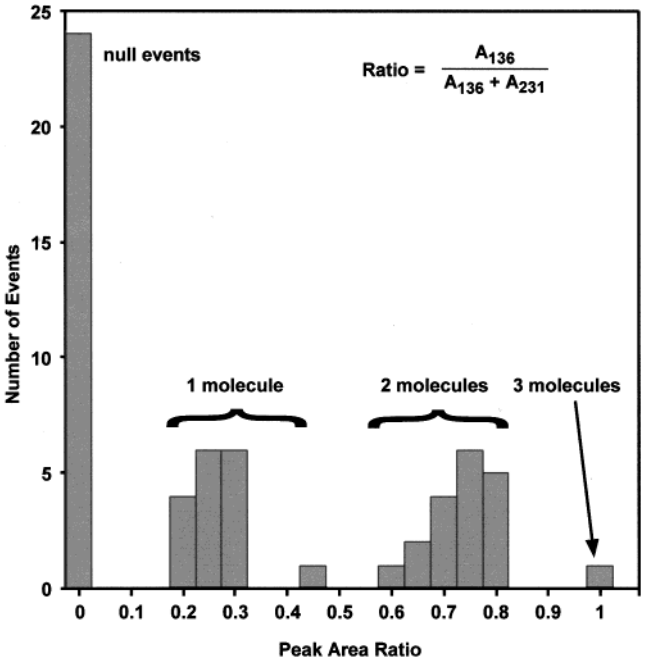

Figure 3. Plot of the number of events as a function of the normalized peak area ratios. The events at 0 represent null events where no 136-bp amplification was seen. The second cluster of events occurs at 0.2−0.4 and represents amplifications from single molecules. The third cluster occurs from 0.6 to 0.8 and represents amplifications from two molecules in the chamber. The last event at 1.0 is likely to be an amplification from 3 molecules in the reactor.

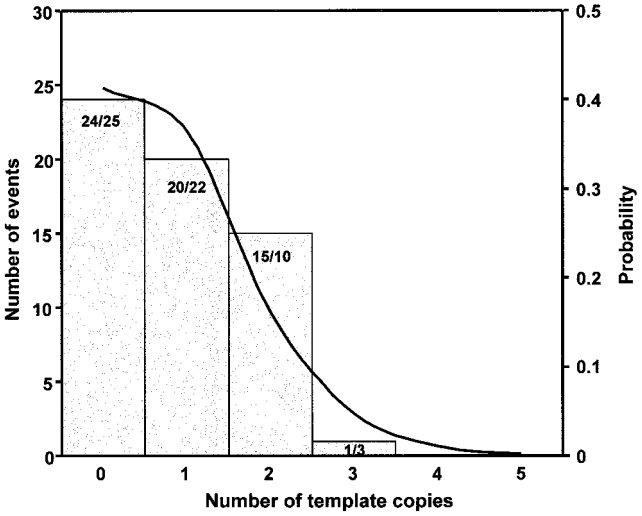

Figure 4. Plot of the number of amplification events observed as a function of the number of template copies in the chamber at the start of PCR amplification. The overlaid curve is the best-fit Poisson function, which has a mean λ of 0.88 molecule. The ratios within each bar are the number of observed events over the number of expected events from the Poisson fit.

of relative peak area is an indication of the relative amounts of material present and will be proportional to the initial number of target molecules present. The normalized peak area ratio $A_{136}/(A_{136} + A_{231})$ is unitless, bounded from 0 to 1, and should demonstrate quantile clusters around particularly frequent events.

Figure 3 presents a graph of the number of events (total 60) as a function of the normalized peak area ratio. Three distinct clusters can be seen; the first, at zero, is the collection of "null events" where no 136-bp peak was observed, the second cluster appears from 0.2 to 0.4, and the third cluster appears from 0.6 to 0.8. Note in particular the absence of events between these clusters, indicating that we are observing quantum fluctuations in the number of template molecules in the reactor. These data strongly suggest that the clusters arise from amplifications of 0, 1, and 2 molecules in the reactor. Varying injection efficiency or disproportional changes in the amplification efficiency of the M13 and S65C control templates would result in a more continuous distribution of relative peak areas; the fact that this is not observed indicates that these phenomena have at most a minimal effect on the results. These data were compared to the presumptive Poisson distribution by grouping into classes of 0, 1, 2, or 3 template copies, based on the clusters of peak area ratios seen in Figure 3. The single event at 0.95 is counted here as the only amplification from 3 molecules.

Figure 4 presents a histogram of the number of events seen with the assumption that single-molecule events fall in the range 0.1−0.5, two-molecule events in the range 0.5−0.9, and three-molecule events in the range >0.9. The observed event frequencies were fit to a Poisson distribution using a log-linear least-squares regression. The resulting maximum likelihood estimates fit is shown overlaid on the data in Figure 4. It has a mean (λ) of 0.88 molecule; testing goodness of fit using χ^2 yielded a value of 0.75 (2 degrees of freedom, $\alpha = 0.05$) and a *p*-value of 0.69, leading us to accept the data as fitting a Poisson distribution. Since calculations of χ^2 for expected event numbers below 5 can lead to erroneous results, goodness of fit was also calculated using the Kolmogorov−Smirnov statistic, which yielded 0.172 ($\alpha = 0.05$, $n = 60$) and a *p*-value of 0.999, strongly indicating the distribution as Poisson. From the serial dilution of the M13 template, we expect 4 copies/μL in the 50-μL mixture, and a 280-nL sample of this stock should result in an average of 1.12 copies in the chamber. The small difference between the expected and observed means could be due to dilution or pipetting error in constructing the stock solution or adsorption of DNA molecules to the pipet/channel walls resulting in lower than expected viable template copies in the reactor.

To test the assumption that the single event at ~1.0 in Figure 3 is an amplification from three molecules, it is necessary to consider the enzymatic efficiencies of both the M13 target and the S65C control. Schnell and Mendoza[33] have expressed the ratio of control to target concentrations at the *n*th cycle of a competitive PCR as

$$\frac{C_n}{T_n} = \frac{[\prod_{i=1}^{n}(1+\epsilon_i')]C_0}{[\prod_{i=1}^{n}(1+\epsilon_i)]T_0}$$

where ϵ_i' and ϵ_i are the amplification efficiencies for the control and target in the *i*th cycle and C_0 and T_0 are the initial control and target concentrations, respectively. In a true competitive PCR, the amplification efficiencies of the target and control are assumed

(33) Schnell, S.; Mendoza, C. *J. Theor. Biol.* **1997**, *184*, 433−440.

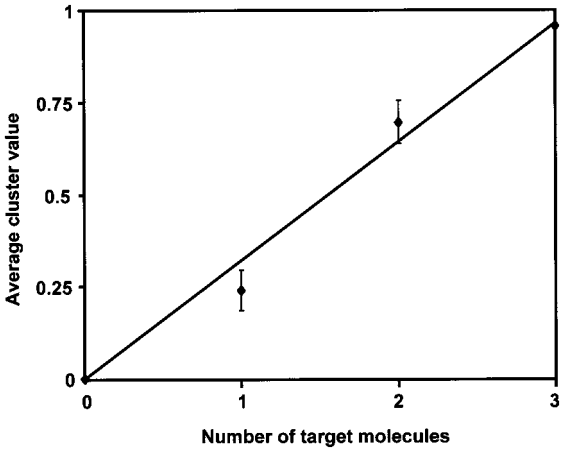

Figure 5. Linear fit of the mean peak area ratio for each cluster seen in Figure 4 versus the assumed number of initial target molecules. The large R^2 value ($R^2 = 0.983$) indicates that, under the assumptions described in the text, the assigned number of initial target molecules in the chamber for each cluster in Figure 4 is accurate.

to be equal, so the ratio of the control to target does not change through time. In our reaction, however, there is no such assumption. The simplest assumption for the functional form of the ratio of efficiencies is linear. This would result in a linear relationship between the peak area ratios in Figure 4 and the number of target molecules in the chamber. Figure 5 presents a linear fit of the mean peak area ratio for each cluster in Figure 4 versus the assumed number of target molecules in the chamber. The fit provides further evidence that the single event at >0.9 is an amplification from 3 target molecules in the chamber.

The molecular detection limits demonstrated here are orders of magnitude better than those achieved previously with microfluidic PCR systems. Our first-generation PCR−CE device, which operated with a 10-μL reactor, required 10^5 starting copies for a successful experiment. Subsequent integrated microdevices[22−24] are also eclipsed by the current system. Microfabricated standalone PCR reactors have also required larger volumes ranging from 500 nL[16] to 28 μL[34] and more initial template copies ranging from ~3000 copies/μL[11] to as high as 10^8 copies/μL.[18] In addition to providing the highest sensitivity, the small reactor volume demonstrated here encourages the construction of integrated parallel analysis systems using this technology.

(34) Taylor, T. B.; Winn-Deen, E. S.; Picozza, E.; Woudenberg, T. M.; Albin, M. *Nucleic Acids Res.* **1997**, *25*, 3164−3168.

SUMMARY AND CONCLUSION

We have observed the stochastic PCR amplification and analysis of single-molecule DNA templates using an integrated glass microdevice. Distinct clusters of 0-, 1-, 2-, and 3-molecule amplification events are observed. The frequencies of these events conform to a Poisson distribution. These observations demonstrate that we are detecting single-molecule amplification events. The ability of our device to amplify single DNA molecules provides an unprecedented molecular limit of detection using microfabricated PCR reactors, and this coupled with the integrated capillary electrophoretic analysis forms the basis of a powerful device for high-sensitivity detection of DNA targets. On one hand, this accomplishment will lead to the development of more complex high-density, low-volume microfluidic diagnostic devices even if they do not operate at the single-molecule limit. On the other hand, single-molecule nucleic acid analyses should facilitate studies of expression from individual cells in a population as well as genetic heterogeneity in cases where population averages mask important biological complexity and variation.

ACKNOWLEDGMENT

Microfabrication of the PCR−CE chip was performed at the UC Berkeley Microfabrication Laboratory. We thank the UC-Berkeley Chemistry Machine Shop for construction of the microfluidic manifolds and the Electronics Shop for electronics fabrication. E.T.L. gratefully acknowledges the support of a Whitaker Foundation Predoctoral Fellowship. This research was supported by the Director, Office of Science, Office of Health and Environmental Research of the U.S. Department of Energy under Contract DE-FG-91ER61125. I.M. is supported by NIH Program Project grant P01 CA77664 in collaboration with Johns Hopkins University.

Received for review August 28, 2000. Accepted November 22, 2000.

AC001026B